ISSN (Print) : 2320 – 3765
ISSN (Online): 2278 – 8875

International Journal of Advanced Research in Electrical, Electronics and Instrumentation Engineering

(An ISO 3297: 2007 Certified Organization)

Vol. 4, Issue 3, March 2015

A New Approach LVRT Control with Enhanced Reactive Power Support for DFIG Wind Turbines

Devalraju Prasad[1], Janapati Balaji[2], N.Sudarshan Rao[3]

Assistant Professor, Dept. of EEE, Narayanadri Institute of Science & Technology, Rajampet, A.P, India[1]

Assistant Professor and HOD, Dept. of EEE, Narayanadri Institute of Science & Technology, Rajampet, A.P, India [2]

Assistant Professor, Dept. of EEE, Narayanadri Institute of Science & Technology, Rajampet, A.P, India[3]

ABSTRACT: The paper presents a new control strategy to enhance the ability of reactive power support of a doubly fed induction generator (DFIG) based wind turbine during serious voltage dips. The proposed strategy is an advanced low voltage ride through (LVRT) control scheme, with which a part of the captured wind energy during grid faults is stored temporarily in the rotors inertia energy and the remaining energy is available to the grid while the DC-link voltage and rotor current are kept below the dangerous levels. After grid fault clearance, the control strategy ensures smooth release of the rotor's excessive inertia energy into the grid. Based on these designs, the DFIG's reactive power capacity on the stator and the grid side converter is handled carefully to satisfy the new grid code requirements strictly. Simulation studies are presented and discussed.

KEYWORDS: Doubly fed induction generator (DFIG), low voltage ride through (LVRT), power system fault, and reactive power.

I.INTRODUCTION

To minimize the negative effects of large-scale wind power integration on the reliability of power grids, different countries have defined different low voltage ride through (LVRT) requirements for wind turbines (WT) in their grid codes. Traditionally, in order to defend the grid against large disturbances on voltage and frequency, traditional thermal generators must fulfill the LVRT requirement as well as providing emergency power supports. With the increased wind penetration, grid connection requirements for WTs are getting reinforced to require reactive power support by WTs during grid faults as well. Doubly fed induction generator (DFIG) based WTs are widely used because of high efficiency, variable speed operation, as well as the use of converters with partial capacity that enables independent control on active and reactive power. To realize LVRT for DFIGs, several technical concerns arisen due to the grid faults must be properly addressed including the over current in the stator and rotor circuits, the overvoltage of the DC-link connecting the rotor side converter (RSC) and the grid side converter (GSC), and the overloading of these converters. To meet the challenging requirements of reactive power support during voltage dips, the reactive power output from DFIGs needs to be increased as much as possible. The existing LVRT solutions for DFIGs can be generally categorized into two types including.

The crowbar protection: Additional crowbar resistors will be inserted into DFIG rotor circuits to limit the over current and the RSC will be disabled temporarily during fault periods. Although the crowbar solution can guarantee successful fault ride through, it will however involve additional investments, energy dissipations by crowbar resistors, and particularly loss of control to active and reactive power outputs. When the crowbar is activated, the DFIG will absorb large amount of reactive power, which can be harmful to the grid.

The demagnetizing method: In order to de- crease rotor current during a fault, demagnetizing methods try to eliminate transients of the induced electromagnetic force in the rotor circuit by controlling the RSC output to trace and counteract the oscillations of stator flux. However, most methods so far are too complicated to be practically implemented by industries. This is mainly due to the limitations in converter capacity, the concerns of the algorithm reliability, and the estimations involved for the control parameters like, e.g., rotor current, rotor flux and rotor voltages, etc.

Recognizing the limitations of existing LVRT solutions, the authors have successfully developed an innovative control strategy featuring improved energy efficiency and algorithm simplicity. By allowing the DFIG rotor to temporarily accelerate, wind energy continuously captured by a WT during a fault can be stored in the rotor as inertia energy, which will be released back to the grid after fault clearance. The simulation results indicate that the method in can decrease the rotor current effectively. Its performance of limiting rotor current is even better than the crowbar protection, not to mention the fact that the latter dissipates the captured wind energy as heats during the faults. Therefore, the method in is considered with high potentials of industrial applications in the future. Focusing on reinforcing the LVRT capability with reactive power supports, this paper will further develop the control strategy in in order to fully utilize a DFIG's potentials to generate power effectively and securely considering a wider range of fault scenarios. Different control schemes can be designed for different voltage stages. At stages of voltage falling and recovering, large rotor or stator current spikes due to electromagnetic transients should be suppressed. At the stage of voltage stabilizing, the basic component of rotor current should be however controlled according to the depth of voltage dip. A staged reactive power controller is proposed to distribute reactive power support between the stator and grid (converter) sides automatically. The proposed control strategy has been implemented using MATLAB/Simulink for a practical 1.5-MW DFIG WT. It has been demonstrated that the new control strategy can fulfill the LVRT requirements and provide enhanced reactive supports to the grid in line with stringent grid code requirements. In addition, simulation results of various test scenarios have not only validated the effectiveness but also the superior performances of the proposed control strategy with respect to both active and reactive power control.

II. MODELING OF A DFIG WIND TURBINE

The schematic diagram of a grid-connected DFIG WT system is shown in Fig.1. The system includes the wind turbine, the shaft system, the induction generator, the back-to-back PWM converters and the control system. Inside the DC-link, a dc-chopper is installed to protect the capacitor and converters from overvoltage. The stator of the induction generator and the grid-side converter are directly connected to the grid synchronously. The control system consists of two subsystems for WT and DFIG respectively.

The WT controller generates the rotor's reference speed based on the optimum power-speed characteristic curve in order to capture maximum wind power, which is termed as maximum power point tracking (MPPT) control. During high winds, the pitch control will ensure the WT working at the rated speed until it is stopped at the cut-off wind speed. Based on vector control techniques, the DFIG controller operates rotor and grid side converters to regulate active and reactive power output of the DFIG independently according to the rotor's reference speed and power factor requirement set by the grid code.

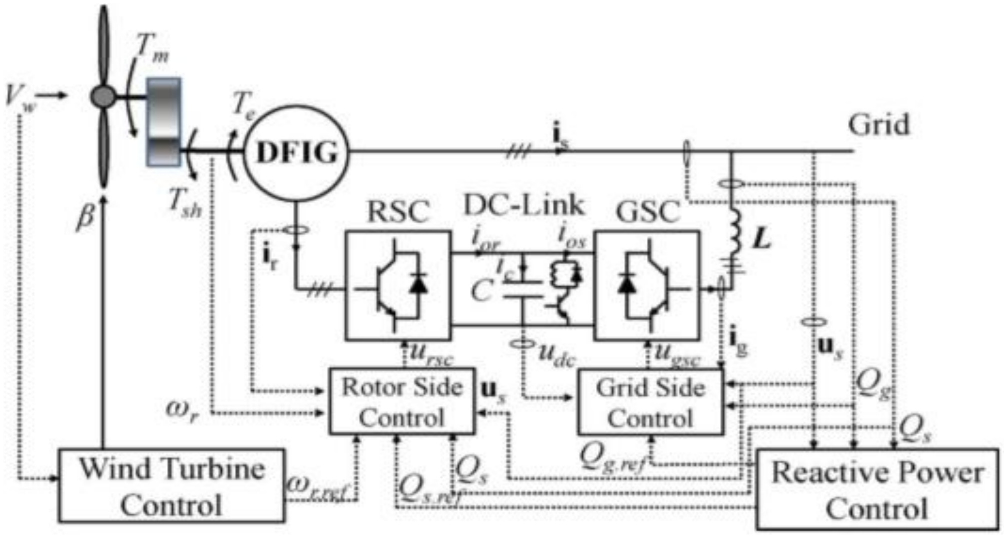

Fig.1. Schematic diagram of a DFIG WT system

III. PROPOSED CONTROL STRATEGY FOR LVRT AND ENHANCED REACTIVE POWER SUPPORT

A power system fault often consists of stages where voltage is falling, stabilizing and recovering, as illustrated in Fig.2. At stage of voltage falling, the curve of rotor current often includes large spikes. At stage of voltage recovering, the transient rotor current is often of high amplitude. Based on this knowledge, special control schemes should be applied and catered for certain stages. The difficulties of LVRT control techniques for DFIG WTs exist in the rapid change of the stator flux caused by the step change of grid voltage. This is the main reason for the observed rotor current oscillations. In view of this, the authors have tried to decrease the basic component of the rotor current through cutting off the energy injection into the rotor circuit in, a different way with practical merits to achieve the same goal of the crowbar protection. Once activated, however, the crowbar protection will convert the DFIG into a typical induction motor.

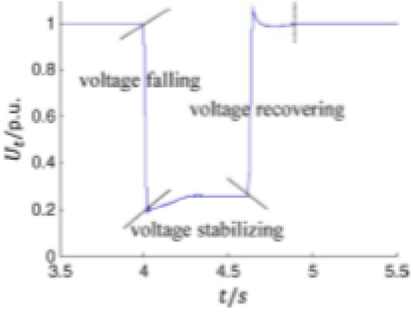

Fig.2. Different stages of voltage development during a typical fault.

Many demagnetizing methods make full use of the control loops for both d- and q-axis currents in the rotor circuit. Compared with these methods, the LVRT control strategy proposed, reserves considerable potential reactive power capacity so that a well-designed reactive controller can largely enhance the reactive power delivery to the grid, which is the focus of this paper. The following sections will introduce the newly proposed control strategy in detail, which integrates the LVRT and reactive power control. Simulation validations as well as comparisons with other existing LVRT and reactive power control methods for DFIGs are given in Section IV.

A. ***Rotor Side Control:*** In normal operations, the decoupling of active and reactive power control is realized through the vector control technique with a reference frame oriented along the stator voltage vector, resulting in the relatively independent d-and q-axis control loops as shown in Fig.3.

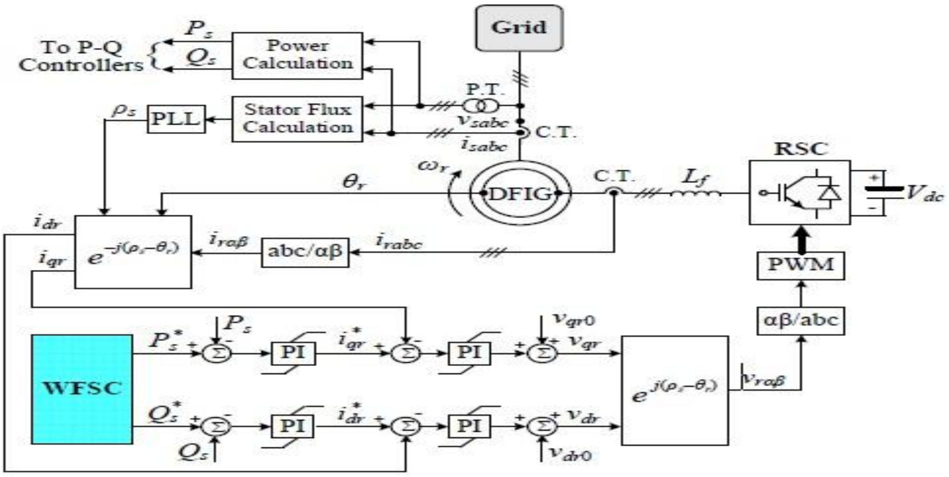

Fig.3. Control scheme of the rotor side converter in normal operations

The q-axis loop controls the electromagnetic torque whose input signal is given by a PI controller comparing the actual rotor speed with the reference one. The d-axis loop, corresponding to the control of magnetizing current, uses the desired reactive power as its input signal. The stator flux in Fig.3 is estimated by the stator voltage.

At the stage of voltage recovering, starting when the voltage at the point of common coupling (PCC) increases above certain threshold, the excess inertia energy is sent out to the grid through a step-change signal given by the speed comparator in the q-axis loop. The stored inertia energy will increase due to the increase of the wind speed, the magnitude of voltage drop, or the fault duration time. The energy released in very short time duration will cause over current if without any special control.

Therefore, the terms and should be decreased in amplitudes at this stage to prevent over current as soon as a voltage recovery is detected. During voltage dips, the power output of a DFIG is certainly decreased. Accordingly the power input should be reduced as well to restore the power balance, which can be done by reducing the electromagnetic torque. Known from Fig.3, the decrease of electromagnetic torque will cause the decrease of q-axis current in the rotor immediately. As a result, the increase of the rotor speed finally absorbs wind energy as the rotor inertia energy during the faults. Ignoring the friction losses, the stored mechanical energy $\Delta E_m(t)$ in the generator rotor at time ***t*** is relevant to the increase of rotor speed and can be expressed as follows:

$$\Delta E_m(t) = \frac{1}{2} J_g [\omega_r (t)^2 - \omega_r (t_{start})^2] \qquad t \geq t_{start} \text{ ....(1)}$$

Where t_{start} is the fault occurrence time, and J_g is the rotor inertia. With high wind speeds, the pitch control will be immediately triggered once the turbine speed exceeds the rated value, so that the captured wind energy will be reduced effectively. Therefore the negative effect of increased mechanical stress to the WT's construction can be little as the pitch control will pre- vent the rotor speed from over-speeding. Under variable speed mode, the MPPT control is realized by setting the generator rotor's reference speed as

$$\omega_{r.ref} = \sqrt[3]{\frac{P_t}{K_{t.opt}}} = \sqrt[3]{\frac{T_t}{K_{t.opt}}} \qquad \text{.......................(2)}$$

Where P_t is the output power, T_t is the electromagnetic torque, and $K_{t.opt}$ is a construction dependent constant. To prevent over current in the stator and rotor, the basic component of active current should be restricted. Accordingly, the maximum allowed active power injected into the generator during a fault is therefore restricted as below, based on (2)

$$P_t \leq \frac{U_s}{U_{s.rated}} . K_{t.opt} \cdot \omega^3_{r.ref} \qquad \text{............................(3)}$$

Where U_s is the RMS value of the current PCC voltage, and $U_{s.rated}$ is the rated value of the voltage. The reference value of q-axis current is expressed as a function of the reference value of electromagnetic torque as in Fig.3

$$I_{qr.ref} = - \frac{L_s}{L_m \psi_s} . T_{e.ref} \qquad \text{............................(4)}$$

The stator flux Ψ_s is hard to be measured accurately, since it changes rapidly and cannot be controlled directly. Equation (4) indicates that this will lead to errors in the reference value for the rotor current. The firstorder partial derivative of $i_{qr.ref}$ on Ψ_s is as follows:

$$\frac{di_{gr.ref}}{d\psi_s} = \frac{L_s}{L_m \psi 2_s} . T_{e.ref} \qquad \text{............................(5)}$$

Because of (5), the impacts due to in accurate stat or flux could be reduced by decreasing the reference torque $T_{e.ref}$, which accordingly slows down the transformation from the mechanical and also magnetic energy to the electrical one in DFIGs. Based on this consideration and (3), the reference value of electromagnetic torque can therefore be derived as

$$T_{e.ref} = \tau \cdot \frac{U_s}{U_{s.rated}} . K_{t.opt} \cdot \omega^3_{r.ref} \quad 0 \leq \tau \leq 1 \qquad \text{...............(6)}$$

Where the factor $\tau \in [1\ 0]$ is determined to effectively suppress the current spikes in the rotor and stator at the stage of voltage falling, and ensure safe LVRT. Considering a large τ may increase the rotor current, the typical value, 0–0.5, is chosen for this stage. At the stage of voltage stabilizing, a too small τ may not ensure the rotor speed within the normal range, especially under the high wind scenarios with the required LVRT duration of more than 1 s with the proposed control, DFIG will continue the active power production during faults. The rotor-side control scheme during voltage dips is illustrated in Fig.4. The new scheme in Fig.4 is still a first-order system. Only the measurements of electric variables e.g. the grid voltage are involved. Though the inertia energy is changing during this control process, there is no inertia response considered, measured or directly controlled. Therefore only a small time delay is possibly involved in the closed control loop. PI controllers with large bandwidths would be better for dealing with the fast oscillations of rotor current during voltage dips. However a larger bandwidth controller often has lower stability. The bandwidth α of a first-order system can be estimated from the 10%–90% rise time t_t as follows: $\alpha = \frac{ln9}{tr}$

In the following simulations, PI controllers with a bandwidth of about 35Hz ,i.e., the risetime of 10ms, are enough to achieve good performances. Similar to the demagnetizing methods, the control performance could also be affected if the voltage magnitude of RSC reaches its limit. Since the proposed method will not fully stop the DFIG from converting the mechanical energy to the electrical one during faults, the RSC voltage limit may not be ex- ceded at all while keeping the rotor current below 2p.u.during the short durations of LVRT.

B. Grid Side Control: The reference frame of the GSC controller is also oriented along the stator voltage vector based on the vector control technique. The d-axis loop controls the active power in order to maintain a stable DC-link voltage. The q-axis loop controls reactive power generated from the grid side as illustrated in Fig.5. Under normal operations, the grid-side circuit current is much smaller than the rotor circuit one. However, the grid side circuit current will rise significantly in low voltage events, where the GSC is an important delivery channel for the remaining active power generated in the rotor circuit, and also a reactive power source. According to Kirchhoff's circuit laws, the DC-link voltage and related branch currents as denoted in Fig. 2, satisfy

$$I_{os} = I_{or} + I_c = I_{or} + C\frac{du_{dc}}{dt} \quad \text{......................(8)}$$

$$I_{or} = \frac{P_r}{u_{dc}} \quad \text{......................(9)}$$

$$I_{dg} = \frac{2\sqrt{2}}{\sqrt{3}\,m}.i_{os} \quad \text{......................(10)}$$

Where i_{os}, i_{or} and i_c are the currents of the three branches connecting the DC-link circuit and the RSC, the GSC and the capacitor C, respectively. i_{dg} is the d-axis component of the grid-side circuit current. U_{dc} is the voltage cross the capacitor C. P_r is the instantaneous active power injecting into the DC-link from the rotor side.m, nominally 0.75, is the factor of PWM modulation depth.

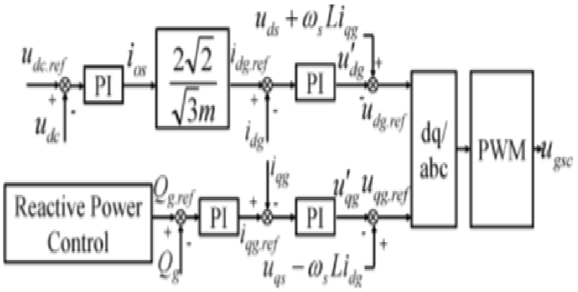

Fig.5. Control scheme of the grid side converter in normal operations

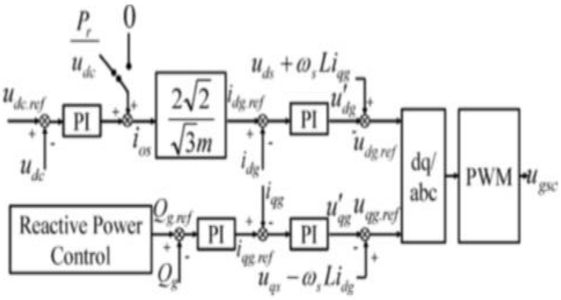

Fig.6. Control scheme of the grid side converter during voltage dips

During voltage dips, intense electromagnetic transients will cause large i_{or}. The PI controller in Fig.5 cannot follow the rapid changes of the current in time. A compensation term is required to be added to represent the instantaneous variations in i_{or}. The term (P_r / U_{dg}) is used as the compensation signal, but the stator voltage may reduce to zero, consequently resulting in overcompensation. Based on (8) and (9), the term (P_r / U_{dc}) is therefore added to the d-axis control loop as shown in Fig.6, in order to smooth the fluctuations of DC-link voltage.

C. Reactive Power Control: Due to limited capacity of DFIG converters, the reactive power reference of the GSC is kept zero in normal operations, in order to decrease the current and losses in both the converters. Meanwhile, the response time of GSC is usually faster than RSC. Therefore, the coordination for reactive power generation between stator and GSC can be realized by using the following staged control scheme, where the output signal of the reactive power controller on the RSC is the input to the one of the GSC. Therefore, the needed reactive power control due to

PCC voltage variations can be distributed automatically between both sides. It firstly uses the RSC to generate reactive power until the fault becomes so serious that the GSC is also required to supply additional reactive power.

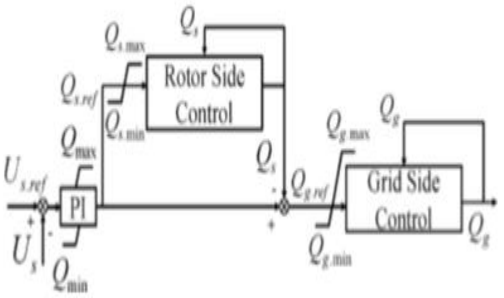

Fig.7. Reactive power control scheme of a DFIG WT

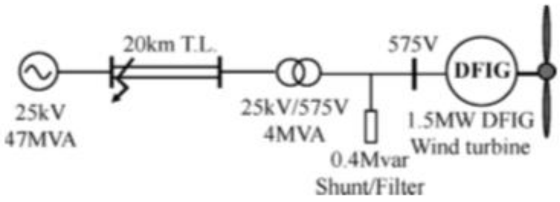

Fig.8. Single line chart of the test system

The LVRT is a sort of power system transient security problems under large disturbances, where voltage drops and needed reactive supports can be uncertain and rather fluctuating. Therefore it is hard to obtain U-Q characteristic curves in advance for power grids during those transients. The curves are often used to determine a schedule to distribute reactive power demands among different control resources in normal operations. Consequently, a PCC-voltage feedback control is proposed for WTs to enhance reactive power support in this paper, as illustrated in Fig.7. In Fig.7 $U_{s.ref}$, denotes the reference RMS value of the PCC voltage. $Q_{s.ref}$ and $Q_{g.ref}$ must be lower than the maximum allowed reactive power of the stator and grid side accordingly

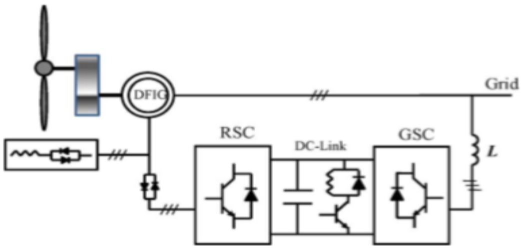

Fig.9. Schematic diagram of the crowbar protection circuit

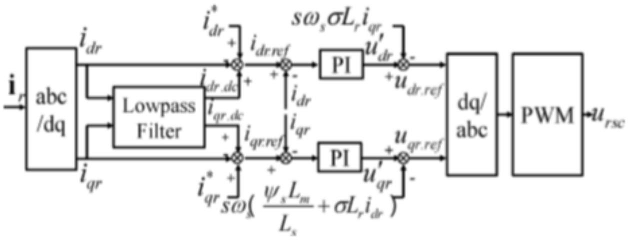

Fig.10.Control scheme of the rotor side converter in Strategy B during voltage dips.

TABLE I
PARAMETER SETTINGS IN THE PROPOSED CONTROL STRATEGY

Parameter	Normal Conditions	Voltage Falling	Voltage Stabilizing	Voltage Recovering
τ	-	0.2	0.5	-
$T_{e.min}$(p.u)	-1.5	-	-	-1.2

IV. SIMULATION RESULTS

As shown in Fig.8, a simple test system has been established consisting of a DFIG and a small transmission system. The DFIG system is based on the models presented in Section II. As shown in Fig.8, a three-phase symmetric fault happens at the location denoted by the arrow, causing voltage dips at the PCC bus. The following simulations were done in the Matlab/ Simulink platform with all models built using standard blocks.

The system performance of the DFIG is shown in Fig.11. In this case, no protection circuit is used during a voltage dip of 60% for 500 ms (Fig.12a). Once the fault occurs at t=3.2 s, the rotor current increases reaching and the peak values of about four times the rated current, and also the DC bus voltage shows a large increase in voltage (Figs.12b-12c).

These severe operating conditions are not acceptable for the power converters. As a first step for reducing the initial peak of the rotor current the effects of crowbar activation is analyzed in case 2

case 1

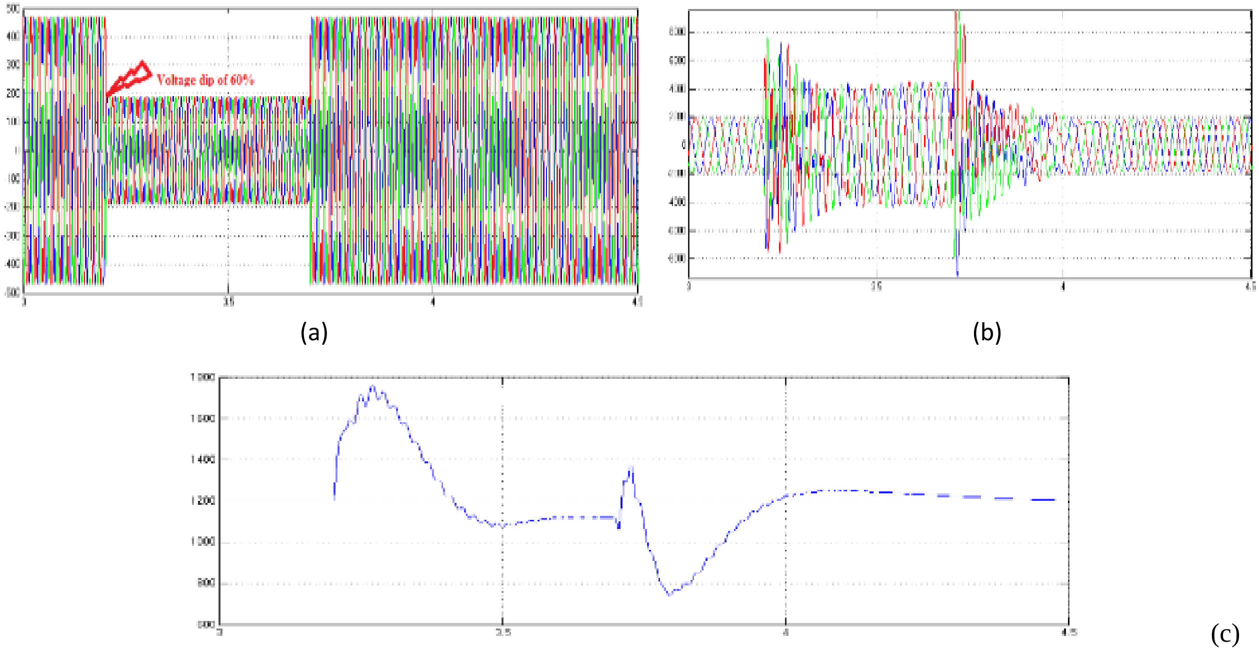

(a) (b)

(c)

Fig.11: Case 1- a) Grid voltage, b) rotor current, c) DC bus voltage.

Case 2

When the fault occurs at t=3.2s, the crowbar is activated and reference values of i_{dr} and i_{qr} are set to zero. After a short transient, the rotor current decreases to zero for the whole period of fault, as represented in Fig.12a. This way it is possible to reduce the rotor current peak, but the DC bus voltage shows the same oscillation as in case 1 (Fig. 12b), and a certain amount of reactive power is absorbed from the grid which deteriorates the stability of the grid (Fig.12c).

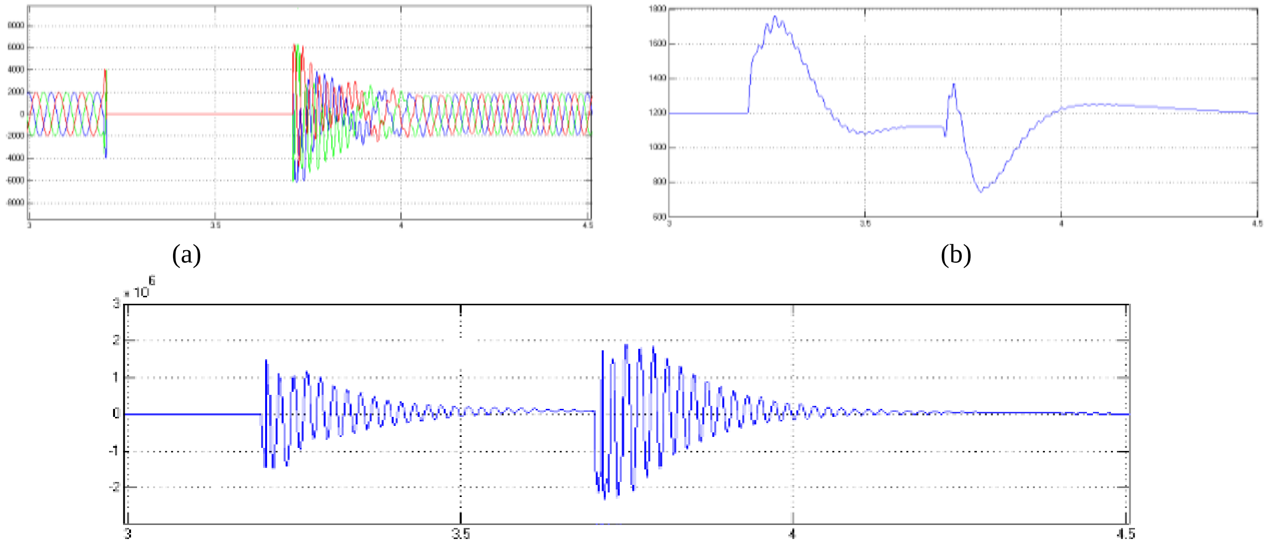

(a) (b)

(c)

Fig.12: Case 2 - a) Rotor current, b) DC bus voltage, c) stator reactive power.

Thus, a new control strategy which can overcome all the disadvantages in case 1 and 2 and meet the grid code requirements is presented and discussed in case3.

Case 3

Fig.13 shows the simulated results of the LVRT operation of the DFIG with the proposed protection strategy. A grid voltage dip of 60% which has duration of 500ms is considered as in cases 1 and 2.

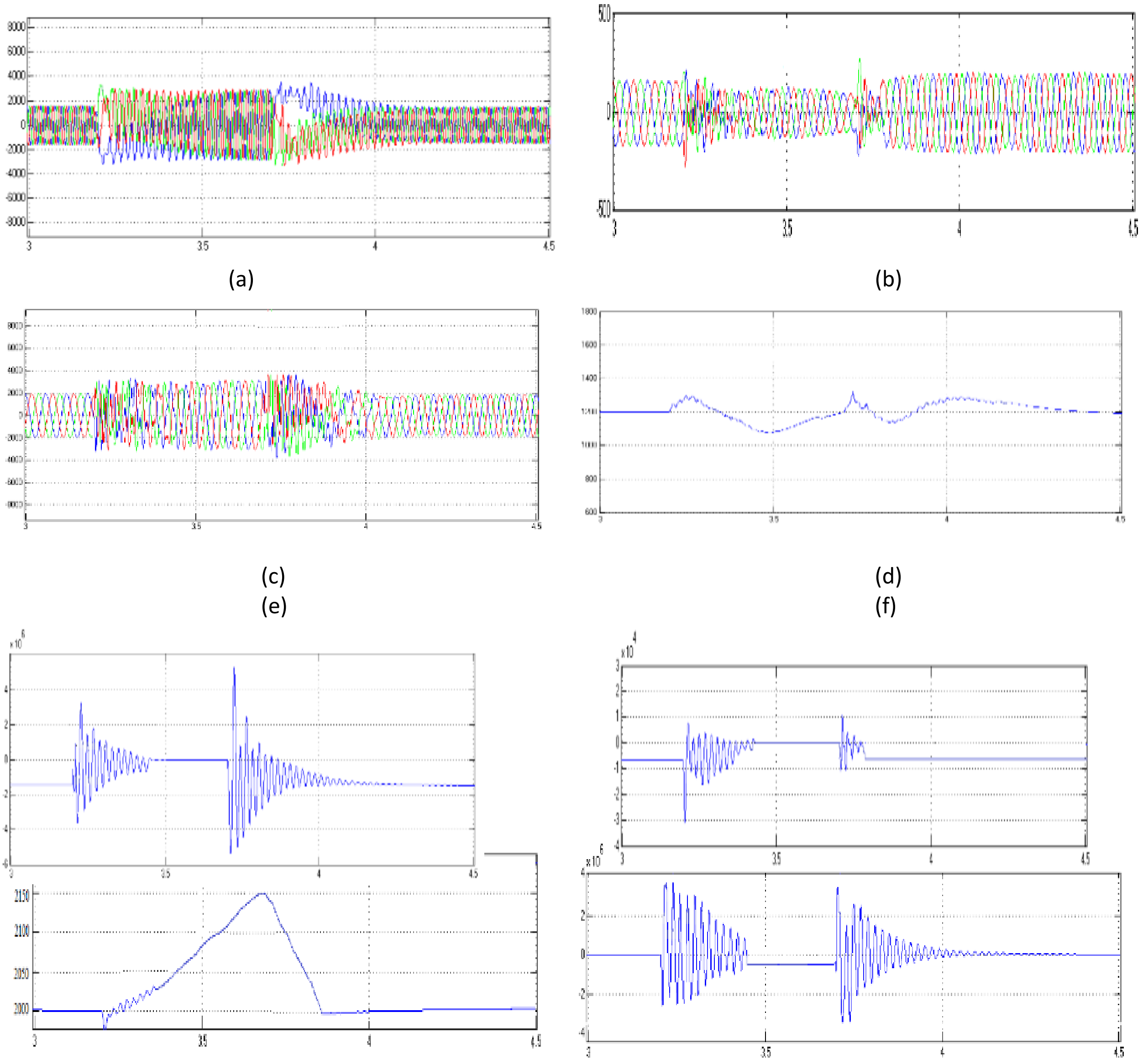

(a) (b)

(c) (d)

(e) (f)

(g) (h)

Fig.13: Case 3 - Crowbar and reactive power control of WECS (a) Stator current, (b) rotor voltage, (c)rotor current, (d) DC bus voltage, (e) generator speed, (f) reactive power, (g) active power, (h) electrictorque, (i) crowbar signal.

Immediately after the fault grid detection, the q-axis rotor current reference is set to zero, and the d-axis rotor current is set to a suitable reference value corresponding to a reactive power of 0.5 MVAR injected into the grid. From the Fig.13, we can see that after a short transient the active power is zero (Fig. 13g), and the reactive power (Fig. 13f) equals the reference value. The reference value of the reactive power should be chosen according to the converter size. As a result, in most time of the voltage dip, the DFIG can supply reactive power to the weak grid, which will increase the grid voltage and help the grid recovery. The DC bus voltage shows lower oscillations with respect cases 1 and 2, as presented in Fig. 10d.The generator speed is given in Fig. 13e, showing a small increase as a consequence of the electromagnetic torque behavior (Fig. 13h). The transient behavior of the stator currents and rotor voltages is characterized by acceptable values and is illustrated in Figs. 13a and 13b, respectively. It can be noted that about 0.2 s after the grid voltage recover, the active power and reactive power resume the reference values as before the fault occurrence. Moreover, with the help of the reactive power, the crowbar does not need to be activated after the clearance of the fault, which means that the rotor side converter can control the DFIG to resume normal operation in less time.

V. CONCLUSION

This paper has been focused on the control strategy of a DFIG wind turbine system equipped with an active crowbar against severe grid faults. In order to reduce the activated time of the crowbar as much as possible, an improved hysteresis control strategy has been proposed. Moreover, the reactive power control has been adopted to decrease the oscillations of the transient current both during the voltage dip and after the clearance of the fault. With the help of the proposed control strategy, the DFIG can be controllable for most of the time during voltage dip. As the crowbar is not required to provide a bypass for the potential high rotor current, the wind turbine can resume normal operation in a few hundred milliseconds after the fault is cleared. Simulation results have shown that an enhanced low voltage ride through capability of the generator can be achieved with the proposed technique.

APPENDIX

The following gives the parameters used in the studied DFIG WT model.
WT: Rated wind speed is 12 m/s; inertia constant H_t = 3s; damping coefficient D_{sh}=0.01 pu; shaft stiffness coefficient K_{sh} =0.5p.u; time constant of the pitch servo T_{servo}=0.25s; DFIG: Base power, voltage and current are 1.5 MW, 575 V and 1505 A accordingly; stator rated voltage and current are 575 V and 1505 A separately; rotor rated voltage and current are 172.5 V and 1505 A accordingly; rotor rated speed is 1.1 p.u. (the synchronous speed is 1 p.u.); inertia constant H_g=0.5s; friction coefficient B=0.01p.u; stator resistance R_s=0.00706p.u; rotor resistance R_r=0.005p.u; stator leakage inductance $L\sigma s$=0.171p.u; rotor leakage inductance $L\sigma r$=0.156p.u; mutual inductance L_m=3.5p.u; the rated voltage on DC-link is 1200 V; the filtering inductance on the grid side L=0.31p.u.

REFERENCES

[1] W. Christiansen and D. R. Johnsen,'' Analysis of Requirements in Selected Grid Codes'', Section of Electric Power Engineering, Technical University of Denmark (DTU), 2006, Tech. Rep.
[2] M. Tsili and S. Papathanassiou, "A review of grid code technical requirements for wind farms," IET Renew. Power Gener., vol. 3, no. 3, pp. 308–332, Mar. 2009.
[3] The Grid Code, no. 4, Rev. 13, National Grid Electricity Transmission plc, U.K., Jun. 2012.
[4] L.Peng,B.Francois,andY.Li,"Improved crowbar control strategy of DFIG based wind turbines for grid fault ride-through," in Proc. IEEE 24th Annual Applied PowerElectronics Conf.Expo.,Washington, DC, USA, Feb. 2009, pp. 1932–1938.
[5] A.H.Kasem, E.F.EI-Saadany,H.H.EI-Tamaly,andM.A.A.Wahab, "An improved fault ride-through strategy for doubly fed induction generator-based wind turbines," IET Renew. Power Gener., vol. 2, no. 4, pp. 201–214, Dec. 2008.
[6] J. López, E. Gubía, E. Olea, J. Ruiz, and L. Marroyo, "Ride through of wind turbines with doubly fed induction generator under symmetrical voltage dips," IEEE Trans. Ind. Electron., vol. 56, no. 10, pp. 4246–4254, Oct. 2009.
[7] M. Kayikçi and J. V. Milanović, "Assessing transient response of DFIG-based wind plants-the influence of model simplifications and parameters," IEEE Trans. Power Syst., vol. 23, no. 2, pp. 545–554, May 2008.

BIOGRAPHY

Devalraju Prasad, born in kumarunipalli, a small village in kadapa district of Andhra Pradesh of south India. He received the B.Tech (E.E.E) degree from Annamacharya Institute of Science and Technology Rajampet and M.Tech (Electrical Power Systems) from Srinivasa Institute of Science Technology, Kadapa, AP, India. Currently, working as an Assistant Professor in Narayanadri Institute Of Science &Technology, Rajampet. He is having 3 years of teaching experience.

Janapati Balaji received the B.Tech (E.E.E) degree from NBKRIST Nellore and M.Tech (Power electronics) from JNTUH, Hyderabad, AP, India. Currently, working as an Assistant Professor and HOD in Narayanadri Institute Of Science &Technology, Rajampet. He is having 10 years of teaching experience.

N.Sudarshan Rao has received the B.Tech (E.E.E) degree from Priyadarshini College of Engineering & Technology, Nellore and M.Tech (Electrical Power Systems) Srinivasa Institute of Technology, Kadapa, AP, India. Currently, working as an Assistant Professor in Narayanadri Institute Of Science &Technology, Rajampet. He is having 3 years of teaching experience.